Article

Not peer-reviewed version

Comprehensive Insight on Regular Damped Oscillatory Structures from Effective Electromagnetic Form Factors Data of Some Mesons and Nucleons

Erik Bartoš , Stanislav Dubnička * , Anna Zuzana Dubničková , Lukáš Holka , Andrej Liptaj

Posted Date: 7 June 2024

doi: 10.20944/preprints202406.0383.v1

Keywords: protons; neutrons; vector mesons; electromagnetic form factors; cross sections; analyticity

Article

Comprehensive Insight on Regular Damped Oscillatory Structures from Effective Electromagnetic form Factors Data of Some Mesons and Nucleons

E. Bartoš[1], S. Dubnička [1,*], A.-Z. Dubničková [2], L. Holka [1], A. Liptaj [1]

[1] Institute of Physics, Slovak Academy of Sciences, Dúbravská cesta 9, SK-84511 Bratislava, Slovak Republic
[2] Department of Theoretical Physics, Comenius University, Bratislava, Slovak Republic
* Correspondence: stanislav.dubnicka@savba.sk

Abstract: We investigate regular damped oscillatory structures appearing in the "effective" form factor of various hadrons. The behavior of this form factor can be extracted from the experimental information on total cross sections, the processes $\sigma_{tot}(e^+e^- \to h\bar{h})$, $h = \pi^{\pm}, K^{\pm}, K^0, p, n$ are examined. The apparent oscillations have been observed for the first time for the proton and we show, taking also other hadrons into the consideration, that they are an arbitrary artifact resulting from a very simplistic theoretical description based on an elementary three-parametric model. If the data are described by a more appropriate and well physically funded U&A model, then the oscillations disappear. In addition, if the simple model is used to describe the data, one observes that the oscillations are opposite for particles which form an isospin dublet. We show, by using the U&A model, that this feature is explained by the transformation properties of the corresponding states in the isotopic space.

Keywords: protons; neutrons; vector mesons; electromagnetic form factors; cross sections; analyticity

1. Introduction

The electromagnetic (EM) structure of any hadron is completely described by the corresponding EM form factors (FFs), the number of which depends on the spin of the considered hadron. Their behaviors in the timelike region can be in principle obtained from the measured total cross sections $\sigma_{tot}(e^+e^- \to h\bar{h})$.

However, there is an essential difference between the charged pion, the charged and neutral K-mesons with the spin "0", the proton and neutron with the spin "1/2", and the deuteron with the spin "1". Whereas the EM structure of the mesons with the spin "0" is completely described by only one EM FF, in the case of the octet of baryons, like the proton and neutron, the complete description of their EM structure requires two different EM FFs, the electric $G_E(s)$ and the magnetic $G_M(s)$. In the case of the deuteron three FFs are needed, the electric, the magnetic and the quadrupole FF. When several form factors are involved, these can not be determined only from the measured total cross section $\sigma_{tot}(e^+e^- \to h\bar{h})$ as function of the total c.m. energy squared "s".

Almost one decade ago new phenomenon appeared [1] in the elementary particle physics, the so-called "regular damped oscillatory structures" (RDOS) from the "effective" proton EM FF data to be obtained from the data on the total cross section $\sigma_{tot}(e^+e^- \to p\bar{p})$. After a couple of years new data on the process $e^+e^- \to n\bar{n}$ with the neutrons have been measured [2] in a rather broad region of energies too, and also in this case RDOS have been revealed, however, with just opposite behavior. There are conjectures [3] that the origin of RDOS are in the quark gluon structure of the protons and neutrons.

This initiated investigations of RDOS also from existing data on the EM structure of the charged pion [4] and the charged and neutral K-mesons [5]. We do not investigate the RDOS of the deuteron here as the experimental data on the total cross section $\sigma_{tot}(e^+e^- \to d\bar{d})$ are still missing.

Further, we try to investigate all these results from the one uniform point of view.

The EM structure of any hadron "h" is completely described by the corresponding EM FFs. In the timelike region their behaviors are experimentally investigated by the measurement of the total cross section of $\sigma_{tot}(e^+e^- \to h\bar{h})(s)$ as a function of the c.m. energy squared "s" on electron-positron colliders. However, the extraction of the absolute values of EM FF behaviors from such total cross

 doi:10.20944/preprints202406.0383.v1

section data is not straightforward in all considered cases and depends on the spin of the investigated hadron.

If the investigated objects are mesons with the spin 0, then there is only one EM FF completely describing their EM structure and the calculation of the absolute value of the EM FF behaviors from the cross section is carried out without any problem.

Nevertheless, if the investigated hadron is the proton or neutron with the spin 1/2, completely described by two EM FFs, the electric $G_E^N(s)$ and the magnetic $G_M^N(s)$ one, one is unable to determine the values of these two independent FFs from one value of the measured total cross section

$$\sigma_{tot}(e^+e^- \to p\bar{p}) = \frac{4\pi\alpha^2 C_p \beta_p(s)}{3s}\left[|G_M^p(s)|^2 + \frac{2m_p^2}{s}|G_E^p(s)|^2\right], \tag{1}$$

or

$$\sigma_{tot}(e^+e^- \to n\bar{n}) = \frac{4\pi\alpha^2 \beta_n(s)}{3s}\left[|G_M^n(s)|^2 + \frac{2m_n^2}{s}|G_E^n(s)|^2\right], \tag{2}$$

with $\beta_N(s) = \sqrt{1-\frac{4m_N^2}{s}}$ the velocity of the outgoing nucleon in the c.m. system, α=1/137 and $C_p = \frac{\pi\alpha/\beta_p(s)}{1-\exp(-\pi\alpha/\beta_p(s))}$ the so-called Sommerfeld-Gamov-Sakharov Coulomb enhancement factor [6]. Therefore the new concept of the "effective" EM FF of the nucleons

$$G_{eff}^p(s) = \sqrt{\frac{\sigma_{tot}^{bare}(e^+e^- \to p\bar{p})}{\frac{4\pi\alpha^2 C_p\beta_p(s)}{3s}\left(1+\frac{2m_p^2}{s}\right)}}, \tag{3}$$

and

$$G_{eff}^n(s) = \sqrt{\frac{\sigma_{tot}^{bare}(e^+e^- \to n\bar{n})}{\frac{4\pi\alpha^2 \beta_n(s)}{3s}\left(1+\frac{2m_n^2}{s}\right)}}, \tag{4}$$

respectively, has been introduced by extending, in a somewhat unnatural way, the equality $G_E^N(s) = G_M^N(s)$, which is exactly valid only at the threshold, to all "s" up to $+\infty$, with the hope of obtaining at least some information on the EM structure of the investigated object.

Further in this paper we investigate both nucleons and the $\pi^\pm, K^\pm, K^0$ mesons.

2. Regular Damped Oscillatory Structures in the Proton "Effective" EM FF

Immediately after publishing the first proton "effective" EM FF data [7,8], obtained by the relation (3) from the measured total cross section (1) by the initial state radiation (ISR) technique, the authors of the paper [1] have described them by the three-parametric formula [9]

$$G_{eff}(s) = \frac{A}{(1+\frac{s}{m_a^2})(1-\frac{s}{0.71})^2}. \tag{5}$$

Then, by a subtraction of the fitted curve from these data, taking errors into account, they have revealed for the first time the RDOS.

We have repeated the latter procedure, collecting all existing data on the proton"effective" FF [7,8,10–13] as presented in Figure 1a, and describing them by the three parametric formula (5) (see Figure 1b) with parameter values $A = 9.02 \pm 0.40$ and $m_a^2 = 8.52 \pm 0.97$ GeV^2 and χ_1^2/ndf=4.61.

 doi:10.20944/preprints202406.0383.v1

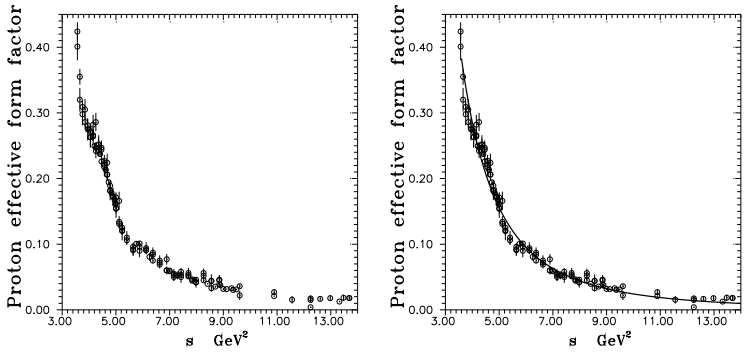

Figure 1. Proton "effective" EM FF data Figure 1a and their description Figure 1b with (5).

Finally, subtracting the fitted curve in Figure 1b from the proton's "effective" EM FF data with errors, RDOS, first time revealed in [1], are confirmed in Figure 2.

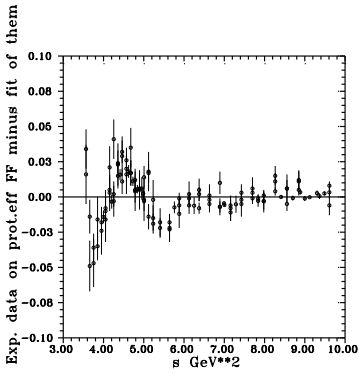

Figure 2. Regular damped oscillatory structures from proton "effective" EM FF experimental data when described by a three-parameter function [9].

3. Regular Damped Oscillatory Structures in the Neutron "Effective" EM FF

After publishing the first neutron "effective" EM FF data [2] in Figure 3a, obtained by the relation (4) from the measured total cross section (2), our description of these data by the three-parametric formula (5) of [9] has not been successful.

In the description of the neutron "effective" FF data from the paper [2] by the three-parameter function (5) of the authors [9] the parameter m_a^2 has been growing to boundless values, indicating its unimportant role for a satisfactory description of the data under consideration. Therefore we have excluded the term $(1 + s/m_a^2)$ from (5) and in the remaining expression only the parameters A(1)=A, and A(3)=0.71, have been left to be free in the fitting procedure. Then the values $A(1) = 0.0698 \pm 0.0060$ and $A(3) = 2.6079 \pm 0.0493$ GeV^2 lead to the description of the data on the neutron "effective" EM FF data in Figure 3a with χ^2/ndf=482/16, as presented by the curve of the Figure 3b.

Then the subtraction of the fitted curve from the data in Figure 3a has revealed the RDOS from the neutron "effective" EM FF data as presented in Figure 4, indicating just an opposite behavior to the RDOS from the proton "effective" EM FF data. This interesting phenomenon will be elucidated later on.

Preprints.org (www.preprints.org) | NOT PEER-REVIEWED | Posted: 7 June 2024 doi:10.20944/preprints202406.0383.v1

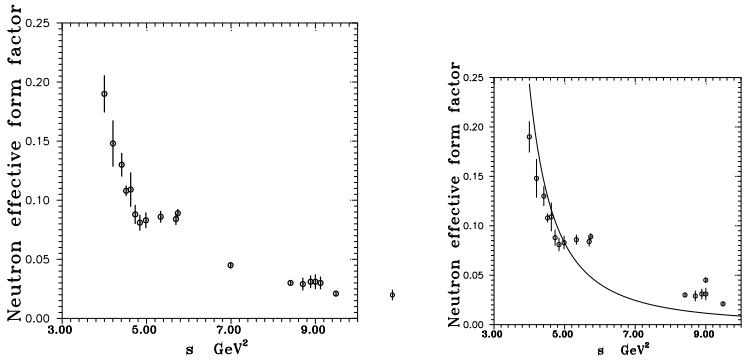

Figure 3. Neutroton "effective" EM FF data Figure 3a and their description Figure 3b with two-parametric function.

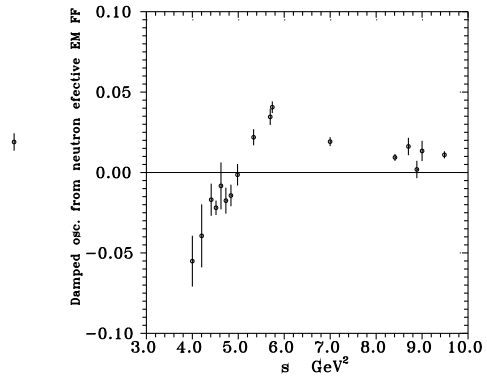

Figure 4. Damped oscillatory regular structures from the neutron's "effective" EM FF experimental data in Figure 3a to be described by a two-parameter function.

4. Search for Regular Damped Oscillatory Structures in Charged Pion EM FF Data

The timelike data on the charged pion EM FF $F_\pi^c(s)$ with errors are hidden in the measured total cross section $\sigma_{tot}^{bare}(e^+e^- \to \pi^+\pi^-)$. We again would like to point out that when obtaining $|F_\pi^c(s)|$ from $\sigma_{tot}^{bare}(e^+e^- \to \pi^+\pi^-)$ no unphysical demands are needed (contrary to the nucleon "effective" FF data), because there is only one function $|F_\pi^c(s)|$ completely describing the measured total cross section which is identified with the pion "effective" EM FF.

However, we meet another problem here. The charged pion EM FF $F_\pi^c(s)$ represents the $\gamma\pi^+\pi^-$ vertex generated by the strong interactions and not all of $\pi^+\pi^-$ pairs in the measured total cross section $\sigma_{tot}^{bare}(e^+e^- \to \pi^+\pi^-)$ have strong interaction origin. Some part of them appears due to electromagnetic isospin violating decay of $\omega(782) \to \pi^+\pi^-$ responsible for a deformation of the right wing of the $\rho(770)$ meson peak, well known as the $\rho - \omega$ interference effect. Since we are investigating oscillatory structures proper to the EM FFs, one has to get rid of the EM isospin violating decay contribution from $\omega(782) \to \pi^+\pi^-$, which can not be made by experimentalists.

In the three most precise measurements till now [14–16] of the total cross section $\sigma_{tot}^{bare}(e^+e^- \to \pi^+\pi^-(\gamma))$ with the initial state radiation (ISR) method, covering the energy range from the threshold up to 9 GeV^2, the following procedure to eliminate the $\omega(782) \to \pi^+\pi^-$ contribution has been applied [4].

First, the total cross section of the $e^+e^- \to \pi^+\pi^-$ process is expressed by means of the sum of $F_\pi^c(s)$ and the isospin violating $\omega(782) \to \pi^+\pi^-$ decay contribution (further denoted by $F_\pi^{'}(s)$) in the form

$$\sigma_{tot}^{bare}(e^+e^- \to \pi^+\pi^-) = \frac{\pi\alpha^2\beta_\pi^3(s)}{3s}|F_\pi^c(s) + Re^{i\phi}\frac{m_\omega^2}{m_\omega^2 - s - im_\omega\Gamma_\omega}|^2, \quad (6)$$

 doi:10.20944/preprints202406.0383.v1

where $F_\pi^c(s)$ is just the pure isovector charged pion EM FF to be expressed by the physically well founded Unitary and Analytic (U&A) model given by the formula (3.66) from [17]

$$\begin{aligned} F_\pi^{th}[W(s)] &= (\frac{1-W^2}{1-W_N^2})^2 \frac{(W-W_Z)(W_N-W_P)}{(W_N-W_Z)(W-W_P)} \\ &\times [\frac{(W_N-W_\rho)(W_N-W_\rho^*)(W_N-1/W_\rho)(W_N-1/W_\rho^*)}{(W-W_\rho)(W-W_\rho^*)(W-1/W_\rho)(W-1/W_\rho^*)} (\frac{f_{\rho\pi\pi}}{f_\rho}) \\ &+ \sum_{v=\rho',\rho'',\rho'''} \frac{(W_N-W_v)(W_N-W_v^*)(W_N+W_v)(W_N+W_v^*)}{(W-W_v)(W-W_v^*)(W+W_v)(W+W_v^*)} (\frac{f_{v\pi\pi}}{f_v})]. \end{aligned} \tag{7}$$

It respects all well known properties of the isovector EM FF of the charged pion, like the analytic behavior with two square-root type branch point approximation, first branch point at the lowest threshold $s_0 = 4m_\pi^2$ and the second s_{in} effectively representing all higher contributions from inelastic processes. The latter is a free parameter of the model, numerically evaluated in a fitting procedure of existing data.

$$W(s) = i \frac{\sqrt{(\frac{s_{in}-s_0}{s_0})^{1/2} + (\frac{s-s_0}{s_0})^{1/2}} - \sqrt{(\frac{s_{in}-s_0}{s_0})^{1/2} - (\frac{s-s_0}{s_0})^{1/2}}}{\sqrt{(\frac{s_{in}-s_0}{s_0})^{1/2} + (\frac{s-s_0}{s_0})^{1/2}} + \sqrt{(\frac{s_{in}-s_0}{s_0})^{1/2} - (\frac{s-s_0}{s_0})^{1/2}}} \tag{8}$$

is the conformal mapping of the four sheeted Riemann surface in s variable into one W-plane,

$$W_N = W(0) = i \frac{\sqrt{(\frac{s_{in}-s_0}{s_0})^{1/2} + i} - \sqrt{(\frac{s_{in}-s_0}{s_0})^{1/2} - i}}{\sqrt{(\frac{s_{in}-s_0}{s_0})^{1/2} + i} + \sqrt{(\frac{s_{in}-s_0}{s_0})^{1/2} - i}} \tag{9}$$

is the normalization point in W-plane and

$$W_v = W(s_v) = i \frac{\sqrt{(\frac{s_{in}-s_0}{s_0})^{1/2} + (\frac{s_v-s_0}{s_0})^{1/2}} - \sqrt{(\frac{s_{in}-s_0}{s_0})^{1/2} - (\frac{s_v-s_0}{s_0})^{1/2}}}{\sqrt{(\frac{s_{in}-s_0}{s_0})^{1/2} + (\frac{s_v-s_0}{s_0})^{1/2}} + \sqrt{(\frac{s_{in}-s_0}{s_0})^{1/2} - (\frac{s_v-s_0}{s_0})^{1/2}}} \tag{10}$$

is a position of poles corresponding to all isovector vector resonances forming the model (7).

A normalization of the model to the electric charge leads to a reduction of the number of free coupling constant ratios $(f_{v\pi\pi}/f_v)$ in (7) and the isovector nature implies that only the rho-meson and its excited states, i.e. $\rho(770), \rho'(1450), \rho''(1700)$ [18] and also the hypothetical $\rho'''(2150)$ [19] can contribute to the FF behavior, in order to cover the energetic region of the data up to 9 GeV^2. The reality condition $F_\pi^*(s) = F_\pi(s^*)$ leads to the appearance of two complex conjugate rho-meson poles on unphysical sheets. The behavior on left-hand cut of the second Riemann sheet, as given by the analytic continuation of the elastic FF unitarity condition [20], is approximated by a Padé approximant, i.e. by one pole W_P and one zero W_Z which are understood as free parameters.

Further in (6) $\phi = \arctan \frac{m_\omega \Gamma_\omega}{m_\rho^2 - m_\omega^2}$ is the $\rho - \omega$ interference phase and R is the real $\rho - \omega$ interference amplitude.

In order to find out optimal parameters, an analysis of existing data in [14–16] on $|F_\pi^{'}(s)|^2$ has been carried out and the obtained results are presented numerically in Table I.

Table 1. Parameter values of the analysis of data in [14–16] with minimum of $\chi^2/ndf = 0.988$.

$s_{in} = 1.2730 \pm 0.0130$[GeV^2]	$m_\rho = 0.7620 \pm 0.0080$[GeV]	$\Gamma_\rho = 0.1442 \pm 0.0014$[GeV]
$(f_{\rho'\pi\pi}/f_{\rho'}) = -0.0706 \pm 0.0012$	$m_{\rho'} = 1.3500 \pm 0.0110$[GeV]	$\Gamma_{\rho'} = 0.3320 \pm 0.0033$[GeV]
$(f_{\rho''\pi\pi}/f_{\rho''}) = 0.0580 \pm 0.0010$	$m_{\rho''} = 1.7690 \pm 0.0180$[GeV]	$\Gamma_{\rho''} = 0.2531 \pm 0.0025$[GeV]
$(f_{\rho'''\pi\pi}/f_{\rho'''}) = 0.0021 \pm 0.0005$	$m_{\rho'''} = 2.2470 \pm 0.0110$[GeV]	$\Gamma_{\rho'''} = 0.0700 \pm 0.0007$[GeV]
$R = 0.0113 \pm 0.0002$	$W_Z = 0.2845 \pm 0.0033$	$W_P = 0.3830 \pm 0.0060$

Now, in order to obtain the values of the pure isovector charged pion EM FF timelike data, the absolute value squared of (6) is expressed as a product of the complex and the complex conjugate terms

 doi:10.20944/preprints202406.0383.v1

$$|F_\pi^c(s)+Re^{i\phi}\frac{m_\omega^2}{m_\omega^2-s-im_\omega\Gamma_\omega}|^2=\{F_\pi^c(s)+Re^{i\phi}\frac{m_\omega^2}{m_\omega^2-s-im_\omega\Gamma_\omega}\}.\{F_\pi^{c*}(s)+Re^{-i\phi}\frac{m_\omega^2}{m_\omega^2-s+im_\omega\Gamma_\omega}\}.$$

By using expressions $F_\pi^c(s)=|F_\pi^c(s)|e^{i\delta_\pi}$, $F_\pi^{c*}(s)=|F_\pi^c(s)|e^{-i\delta_\pi}$ and the identity between the pion EM FF phase and the P-wave isovector $\pi\pi$-phase shift $\delta_\pi(s)$=$\delta_1^1(s)$, which follows from the charge pion EM FF elastic unitarity condition, practically considered to be valid up to 1 GeV, the quadratic equation for the absolute value of the pure isovector charged pion EM FF $|F_\pi^c(s)|$ is found

$$|F_\pi^c(s)|^2+|F_\pi^c(s)|\frac{2Rm_\omega^2}{(m_\omega^2-s)^2+m_\omega^2\Gamma_\omega^2}[(m_\omega^2-s)\cos(\delta_1^1-\phi)+m_\omega\Gamma_\omega\sin(\delta_1^1-\phi)]$$
$$+\frac{R^2m_\omega^4}{(m_\omega^2-s)^2+m_\omega^2\Gamma_\omega^2}-\frac{3s}{\pi\alpha^2\beta_\pi^3(s)}\sigma_{tot}^{bare}(e^+e^-\to\pi^+\pi^-)=0. \quad (11)$$

Its solution gives the relation

$$|F_\pi^c(s)|=-\frac{Rm_\omega^2}{(m_\omega^2-s)^2+m_\omega^2\Gamma_\omega^2}[(m_\omega^2-s)\cos(\delta_1^1-\phi)+m_\omega\Gamma_\omega\sin(\delta_1^1-\phi)]$$
$$\pm\{\frac{R^2m_\omega^4}{[(m_\omega^2-s)^2+m_\omega^2\Gamma_\omega^2]^2}[(m_\omega^2-s)\cos(\delta_1^1-\phi)+m_\omega\Gamma_\omega\sin(\delta_1^1-\phi)]^2 \quad (12)$$
$$-\frac{R^2m_\omega^4}{(m_\omega^2-s)^2+m_\omega^2\Gamma_\omega^2}+\frac{3s}{\pi\alpha^2\beta_\pi^3(s)}\sigma_{tot}^{bare}(e^+e^-\to\pi^+\pi^-)\}^{1/2}$$

in which a physical solution is given by the "+" sign of the second term.

We use the most accurate up-to-now $\delta_1^1(s)$ data [21] described by a model independent parametrization [22] with $q=[(s-4m_\pi^2)/4]^{1/2}$ and numerical values of parameters in Table I which provide the best description of $\sigma_{tot}^{bare}(e^+e^-\to\pi^+\pi^-)$ as measured in [14–16]. In this way the information about the absolute value $|F_\pi^c(s)|$ of the pure isovector EM FF of the charged pion with errors is extracted, see Table II, Table III and Table IV of [4], respectively.

All three sets of data on the absolute value $|F_\pi^c(s)|$ of the pure isovector EM FF of the charged pion as a function of s from threshold up to 9 GeV^2 as given in Tables II.–IV. of [4] are graphically presented in Figure 5a.

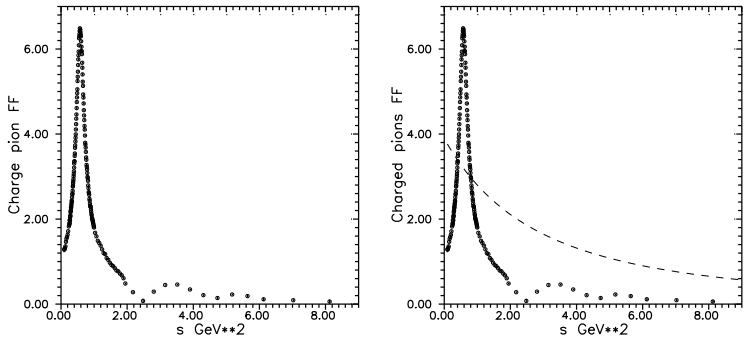

Figure 5. Charged pion "effective" EM FF data Figure 5a and their description in Figure 5b with dashed line given by a formula similar to (5), however now with parameters $\mathbf{A=3.9888\pm0.0061}$, $\mathbf{m_a^2=5.5647\pm0.1915GeV^2}$ and the third parameter to be $\mathbf{A_3=-5.5647\pm0.1037GeV^2}$.

Afterwards these data are, as well as it is possible, described by a similar formula to (5), however, now the nucleon "magic" number 0.71 is substituted by the third free parameter A_3, because one can not expect the nucleon "magic" number to be appropriate also in the pion case.

The best fit of the data in Figure 5 has been achieved with parameter values $\mathbf{A=3.9888\pm0.0061}$, $\mathbf{m_a^2=5.5647\pm0.1915GeV^2}$ and the charged pion "magic" number $\mathbf{A_3=-5.5647\pm0.1037GeV^2}$. The result of the fit is graphically presented in Figure 5b by the dashed line.

Preprints.org (www.preprints.org) | NOT PEER-REVIEWED | Posted: 7 June 2024 doi:10.20944/preprints202406.0383.v1

If dashed line values are subtracted from the experimental values of $|F_\pi^c(s)|$ (Tables II.–IV. of [4]), damped oscillatory structures from the charged pion"effective" EM FF data appear, as it is presented in Figure 6.

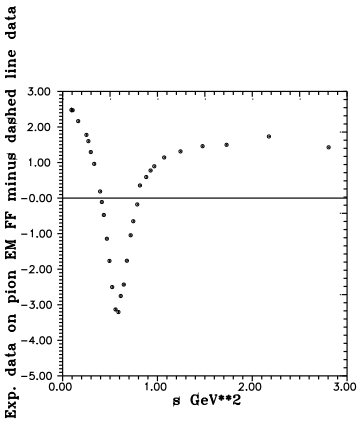

Figure 6. Damped oscillatory structures from the charged pion "effective" EM FF data obtained by a subtraction of dashed line data in Figure 5b from experimental data on $|F_\pi^c(s)|$ in Figure 5a

5. Investigation of Damped Oscillatory Structures from Charged K-Meson EM FF Timelike Data

The timelike data on the charged K-meson EM structure are contained in the measured total cross section $\sigma_{tot}^{bare}(e^+e^- \to K^+K^-)$. To evaluate these data no additional unphysical assumptions are needed because there is only one function $|F_K^{\pm}(s)|$ completely describing the measured total cross section of the electron-positron annihilation into K^+K^- pair. The $|F_K^{\pm}(s)|$ with errors, which is identified with the charged kaon "effective" EM FF, is calculated by means of the following relation

$$G_{eff}^{K^\pm}(s) = |F_{K^\pm}(s)| = \sqrt{\sigma_{tot}^{bare}(e^+e^- \to K^+K^-)\frac{3s}{\pi\alpha^2 C_K{}^{\pm}\beta_K^{3\,\pm}}}, \tag{13}$$

with $\beta_K{}^{\pm}(s) = \sqrt{1-\frac{4m_K^{2\,\pm}}{s}}$, α=1/137 and $C_K{}^{\pm} = \frac{\pi\alpha/\beta_K{}^{\pm}(s)}{1-\exp(-\pi\alpha/\beta_K{}^{\pm}(s))}$ being the so-called Sommerfeld-Gamov-Sakharov Coulomb enhancement factor [6] of charged kaons, which accounts for the EM interaction between the outgoing K^+K^-. The total cross section data we use in (13) will be taken from two recent ISR measurements of the process $e^+e^- \to K^+K^-(\gamma)$, one from [23] for $s < 25$ GeV^2, and another from [24] in the range 6.76 GeV^2 $< s <$ 64 GeV^2. These two data sets are together graphically presented in Figure 7

and the region (2-7) GeV^2 is in more detail shown in Figure 8.

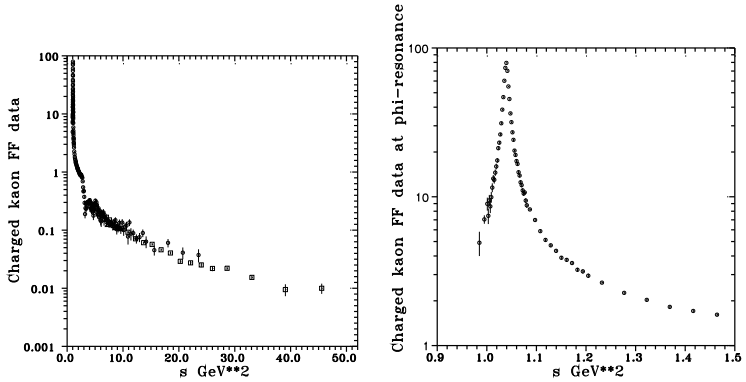

Figure 7. Charged kaon EM FF data $|F_K^{\pm}(s)|$.

Preprints.org (www.preprints.org) | NOT PEER-REVIEWED | Posted: 7 June 2024 doi:10.20944/preprints202406.0383.v1

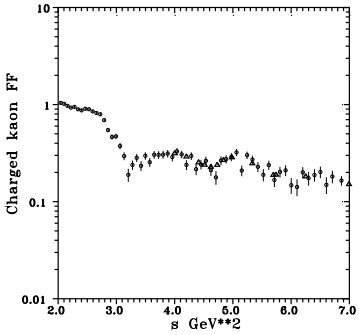

Figure 8. The data on $|F_{K^\pm}(s)|$ in the region 2-7 GeV^2.

As one can see from Figure 7, the data in [23] above 6.5 GeV^2 are very scattered, even in some points inconsistent. As a result it is impossible to achieve a statistically acceptable χ^2/ndf value in the description of such data. Fortunately, the same experimental BABAR group in the paper [24] repeated measurements of the $e^+e^- \to K^+K^-$ process from 6.76 GeV^2 to 64 GeV^2 and obtained more precise and reliable data. Hence we have excluded all data from [23] in the energy range 6.76 GeV^2 - 25 GeV^2 and substituted them by more precise data from [24].

In order to investigate possible oscillatory structure from the charged K-meson EM FF timelike data by using the same procedure as for the proton, the modification of the formula (5) has been made, in the sense that the magic nucleon number 0.71 GeV^2 was left as a free parameter A3 in our analysis. Then the best description of the data in Figure 7 is achieved with A=5.14773 $\pm$ 0.0013 , m_a^2=0.2400 $\pm$ 0.0709 GeV^2 and A3=0.8403 $\pm$ 0.0024 GeV^2, as it is graphically presented in Figure 9 by the dashed line. If dashed curve data are subtracted from selected charged K-meson FF data, RDOS are observed around the line crossing the zero as seen in Figure 10.

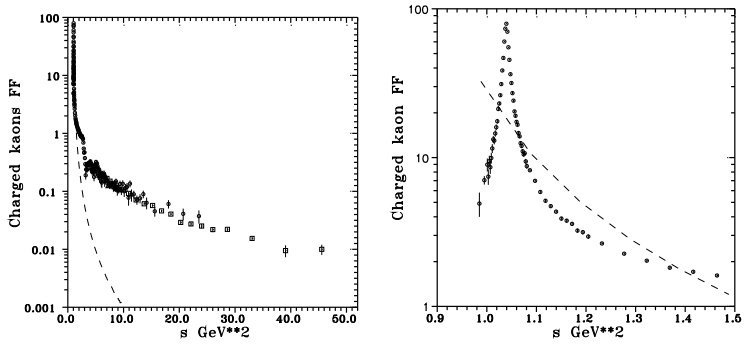

Figure 9. Charged kaon EM FF data described by dashed line as generated by the modified three parametric formula (5).

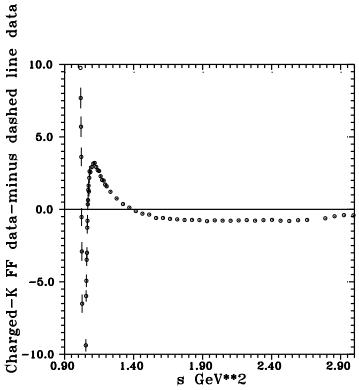

Figure 10. Damped oscillatory structures revealed by a subtraction of dashed line data in Figure 7 from selected $|F_{K^\pm}(s)|$ data with errors.

 doi:10.20944/preprints202406.0383.v1

6. Investigation of Damped Oscillatory Structures from Neutral K-Meson EM FF Timelike Data

The timelike data on the neutral K-meson EM FF $|F_{K^0}(s)|$, which completely describes the neutral K-meson EM structure, can be obtained from the measured total cross section $\sigma_{tot}^{bare}(e^+e^- \to K_S K_L)$, which is, however, more difficult to be measured than $\sigma_{tot}^{bare}(e^+e^- \to K^+K^-)$. As a result one can expect also that the obtained experimental information on $|F_{K^0}(s)|$ will be of a lower quality than the data on $|F_K^{\pm}(s)|$.

According to our knowledge there are no data on the function $|F_{K^0}(s)|$ with errors published during the last decade, nevertheless we have calculated them in the paper [5] by means of the relation

$$G_{eff}^{K^0}(s) = |F_{K^0}(s)| = \sqrt{\sigma_{tot}^{bare}(e^+e^- \to K_S K_L)\frac{3s}{\pi\alpha^2\beta_{K^0}^3}} \tag{14}$$

with $\beta_{K^0}(s) = \sqrt{1 - \frac{4m_{K^0}^2}{s}}$, α=1/137, from one recent measurement [25] of the process $e^+e^- \to K_S K_L(\gamma)$ by the ISR technique in the interval of energy values s (1.1664-4.84) GeV^2 and from two measurements [26], [16] by the scan method, the first one in the ϕ-resonance region (1.0080-1.1236) GeV^2 and the second in the range of energies (4.0000-9.4864) GeV^2. This second measurement is the first measurement that has probed this interval of energies. Their numerical values with errors are given in Table II and graphically presented in Figure 11.

Table 2. The data on $|F_{K^0}(s)|$ with errors.

s [GeV^2]	$\lvert F_{K^0}(s)\rvert \pm err.$	s [GeV^2]	$\lvert F_{K^0}(s)\rvert \pm err.$	s [GeV^2]	$\lvert F_{K^0}(s)\rvert \pm err.$	s [GeV^2]	$\lvert F_{K^0}(s)\rvert \pm err.$
1.0080	11.4683 ± 0.3506	1.0588	16.7599 ± 0.1729	1.9600	0.2369 ± 0.0592	4.2025	0.1120 ± 0.0496
1.0201	19.6100 ± 0.1093	1.0692	10.9758 ± 0.1380	2.0736	0.2821 ± 0.0529	4.4100	0.0829 ± 0.0004
1.0241	27.1841 ± 0.1405	1.0816	07.8863 ± 0.1274	2.1904	0.2968 ± 0.0453	4.4944	0.0713 ± 0.0035
1.0302	36.4652 ± 0.4169	1.1025	05.0943 ± 0.0752	2.3104	0.3999 ± 0.0394	4.6225	0.0653 ± 0.0136
1.0323	45.4557 ± 0.2066	1.1046	05.1158 ± 0.1376	2.4336	0.4022 ± 0.0390	4.7306	0.0748 ± 0.0075
1.0343	57.6351 ± 0.1353	1.1236	03.8750 ± 0.1138	2.5600	0.4505 ± 0.0322	4.8400	0.0738 ± 0.0057
1.0363	70.4012 ± 0.1847	1.1664	02.4831 ± 0.0778	2.6896	0.4488 ± 0.0351	4.9836	0.0876 ± 0.0666
1.0384	81.3097 ± 0.1731	1.2544	01.2826 ± 0.0687	2.8224	0.3531 ± 0.0381	5.3333	0.0716 ± 0.0048
1.0404	77.0351 ± 0.1361	1.3456	00.8939 ± 0.0603	2.9584	0.2534 ± 0.0536	5.6949	0.0342 ± 0.0055
1.0424	59.0975 ± 0.1734	1.4400	00.7436 ± 0.0578	3.0976	0.1659 ± 0.0528	5.7408	0.0367 ± 0.0038
1.0445	48.1169 ± 0.1663	1.5376	00.5341 ± 0.0553	3.2400	0.0872 ± 0.0727	6.9929	0.0437 ± 0.0050
1.0465	37.7921 ± 0.2656	1.6384	00.4013 ± 0.0520	3.3856	0.1015 ± 0.0508	7.0034	0.0455 ± 0.0043
1.0506	26.1639 ± 0.3264	1.7424	00.3877 ± 0.0538	3.5344	0.0724 ± 0.0724	8.4100	0.0253 ± 0.0036
1.0568	18.6920 ± 0.1371	1.8496	00.3253 ± 0.0529	4.0000	0.1223 ± 0.0663	9.4864	0.0257 ± 0.0030

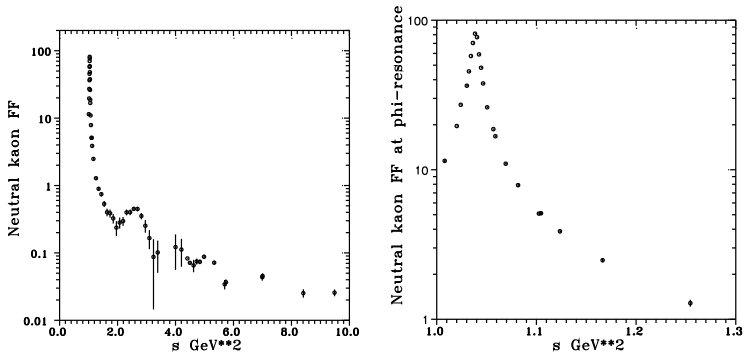

Figure 11. Neutral kaon EM FF data.

In order to study eventual damped oscillatory structures from the neutral K-meson EM FF timelike data by using the same procedure as for the proton, again the modified formula (5) with the third parameter 0.71 GeV^2 to be a free parameter A3 is utilized in a fitting procedure of the data in Figure 11. Their best description has been achieved with parameter values A=0.4729 ± 0.0061,

Preprints.org (www.preprints.org) | NOT PEER-REVIEWED | Posted: 7 June 2024 doi:10.20944/preprints202406.0383.v1

m_a^2=−.9267 ± 0.0016 GeV^2 and A3=0.9269 ± 0.0003 GeV^2 and is graphically presented in Figure 12 by the dashed line.

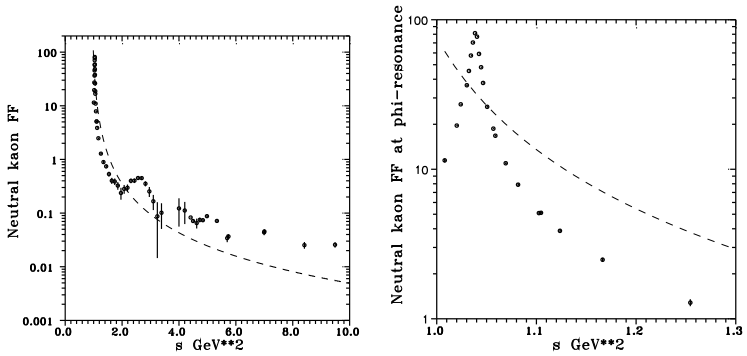

Figure 12. Neutral kaon EM FF data optimally described by dashed line as generated by the modified three parametric formula (5).

If the dashed line is subtracted from the neutral K-meson FF data in Figure 11, taking errors into account, damped oscillatory structures can be observed around the line crossing the zero as depicted in Figure 13.

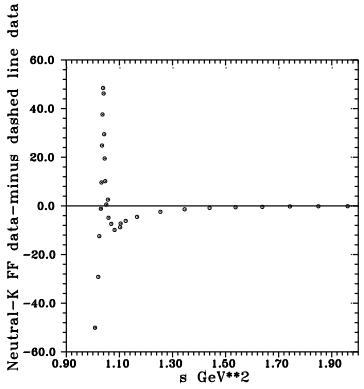

Figure 13. Damped oscillatory structures revealed by a subtraction of dashed line data in Figure 12 from $|F_{K^0}(s)|$ data with errors given in Table II.

Comparing the oscillations depicted in the Figure 10 and in Figure 13 with those of the nucleons in Figure 2 and Figure 4, one finds an analogy between the behaviors of the damped oscillations in the K-meson FF data and those of damped oscillations in the nucleon "effective" EM FF data. In both cases the oscillations in the data for one particle (say the charged K-meson) correspond roughly to the oscillations in the data for its partner particle in the respective isospin doublet (say the neutral K-meson) if reflected through the axis y=0. Where the oscillations for charged kaons have maxima the oscillations for neutral kaons have minima, and vice versa. The same property can be observed in the oscillations of proton and neutron data.

This feature seems to be interesting and it must be explained by some serious physical arguments.

7. Damped Oscillation Structures in the Possible Deuteron "Effective" EM FF Data

The deuteron EM structure is completely described by three independent EM FFs, usually chosen to be the charge $G_C(s)$, the magnetic $G_M(s)$ and the quadrupole $G_Q(s)$ FF. Then, from the total cross

 doi:10.20944/preprints202406.0383.v1

section of the electron-positron annihilation into the deuteron-antideuteron pair expressed as function of EM FFs

$$\sigma_{tot}(e^+e^- \to d\bar{d}) = \frac{\pi\alpha^2\beta_d^3(s)}{3s}\Big(\frac{s}{m_d^2}|G_C(s)+G_M(s)+G_Q(s)|^2 + \tag{15}$$

$$+[2|G_C(s)+\frac{s}{2m_d^2}G_Q(s)|^2+|G_C(s)+\frac{s}{2m_d^2}G_M(s)|^2]\Big) \tag{16}$$

one can see immediately that it is not a simple task to obtain any experimental information on the corresponding deuteron EM FFs in $s > 4m_d^2$ region. With the aim of a obtaining at least some information on the EM structure of the deuteron, one can define the "effective" deuteron EM FF by a requirement of the equality $G_C(s) = G_M(s) = G_Q(s)$ for all $s > 4m_d^2$ up to $+\infty$, like in the case of the nucleons, and in this way obtain data on

$$G_{eff}^d(s) = \sqrt{\frac{s\sigma_{tot}(e^+e^- \to d\bar{d})}{\pi\alpha^2\beta_d^3(s)(\frac{3s}{m_d^2}+|1+\frac{3}{2m_d^2}|^2)}} \tag{17}$$

from experimental data on the $\sigma_{tot}(e^+e^- \to d\bar{d})$. However, the latter are still missing.

8. Origin of the Opposite-Behavior Phenomenon in RDOS of Isodoublets

Investigating the RDOS of nucleons and charged and neutral K-mesons, we have observed that the RDOS of the proton is just opposite to the RDOS of the neutron. The same has been observed in the case of charged and neutral K-mesons.

Next we investigate the latter phenomenon on the isodoublet of the proton and neutron, which could be, in the same way, repeated also in the case of the charged and neutral K-mesons.

The proton and neutron EM FFs in the total cross sections (1) and (2), respectively, and consequently also in (3) and (4), are the Sachs proton electric and proton magnetic FFs, which can be expressed through the Dirac and Pauli EM FFs, to be defined by the parametrization of the matrix element of the nucleon EM current

$$< N|J_\mu^{EM}(0)|N >= e\bar{u}(p')[\gamma_\mu F_1^N(t) + \frac{i}{2m_N}\sigma_{\mu\nu}(p'-p)^\nu F_2^N(t)]u(p), \tag{18}$$

and the latter, taking into account the special transformation properties of the nucleon EM current in the isotopic space, are further split into the same isoscalar and isovector parts for both nucleons, with "+" sign for protons and with the "-" sign for neutrons, as follows

$$G_E^p(t) = F_1^p(s) + \frac{s}{4m_p^2}F_2^p(s) = [F_{1s}^N(t)+F_{1v}^N(t)] + \frac{t}{4m_p^2}[F_{2s}^N(t)+F_{2v}^N(t)], \tag{19}$$

$$G_M^p(t) = F_1^p(s) + F_2^p(s) = [F_{1s}^N(t)+F_{1v}^N(t)] + [F_{2s}^N(t)+F_{2v}^N(t)],$$

and

$$G_E^n(t) = F_1^n(s) + \frac{s}{4m_p^2}F_2^n(s) = [F_{1s}^N(t)-F_{1v}^N(t)] + \frac{t}{4m_n^2}[F_{2s}^N(t)-F_{2v}^N(t)], \tag{20}$$

$$G_M^n(t) = F_1^n(s) + F_2^n(s) = [F_{1s}^N(t)-F_{1v}^N(t)] + [F_{2s}^N(t)-F_{2v}^N(t)].$$

On this place we would like to stress that as a result both, the proton EM FFs (19) and the neutron EM FFs (20) depend on the same physically interpretable free parameters to be determined by fitting

 doi:10.20944/preprints202406.0383.v1

only the existing data on the $\sigma_{tot}(e^+e^- \to p\bar{p})$ by the advanced 9 vector-meson resonance Unitary and Analytic (U&A) model [27] of the nucleon EM structure

$$
\begin{aligned}
F_{1s}[V(s)] = \left(\frac{1-V^2}{1-V_N^2}\right)^4 \Bigg\{ & \frac{1}{2} H_{\omega''}(V) H_{\phi''}(V) \\
& + \Bigg[H_{\phi''}(V) H_{\omega'}(V) \frac{(C^{1s}_{\phi''} - C^{1s}_{\omega'})}{(C^{1s}_{\phi''} - C^{1s}_{\omega''})} + H_{\omega''}(V) H_{\omega'}(V) \frac{(C^{1s}_{\omega''} - C^{1s}_{\omega'})}{(C^{1s}_{\omega''} - C^{1s}_{\phi''})} \\
& \qquad - H_{\omega''}(V) H_{\phi''}(V) \Bigg] (f^{(1)}_{\omega' NN}/f_{\omega'}) \\
& + \Bigg[H_{\phi''}(V) H_{\phi'}(V) \frac{(C^{1s}_{\phi''} - C^{1s}_{\phi'})}{(C^{1s}_{\phi''} - C^{1s}_{\omega''})} + H_{\omega''}(V) H_{\phi'}(V) \frac{(C^{1s}_{\omega''} - C^{1s}_{\phi'})}{(C^{1s}_{\omega''} - C^{1s}_{\phi''})} \\
& \qquad - H_{\omega''}(V) H_{\phi''}(V) \Bigg] (f^{(1)}_{\phi' NN}/f_{\phi'}) \\
& + \Bigg[H_{\phi''}(V) L_{\omega}(V) \frac{(C^{1s}_{\phi''} - C^{1s}_{\omega})}{(C^{1s}_{\phi''} - C^{1s}_{\omega''})} + H_{\omega''}(V) L_{\omega}(V) \frac{(C^{1s}_{\omega''} - C^{1s}_{\omega})}{(C^{1s}_{\omega''} - C^{1s}_{\phi''})} \\
& \qquad - H_{\omega''}(V) H_{\phi''}(V) \Bigg] (f^{(1)}_{\omega NN}/f_{\omega}) \\
& + \Bigg[H_{\phi''}(V) L_{\phi}(V) \frac{(C^{1s}_{\phi''} - C^{1s}_{\phi})}{(C^{1s}_{\phi''} - C^{1s}_{\omega''})} + H_{\omega''}(V) L_{\phi}(V) \frac{(C^{1s}_{\omega''} - C^{1s}_{\phi})}{(C^{1s}_{\omega''} - C^{1s}_{\phi''})} \\
& \qquad - H_{\omega''}(V) H_{\phi''}(V) \Bigg] (f^{(1)}_{\phi NN}/f_{\phi}) \Bigg\}
\end{aligned}
\tag{21}
$$

 doi:10.20944/preprints202406.0383.v1

with 5 free parameters $(f^{(1)}_{\omega' NN}/f_{\omega'}), (f^{(1)}_{\phi' NN}/f_{\phi'}), (f^{(1)}_{\omega NN}/f_{\omega}), (f^{(1)}_{\phi NN}/f_{\phi}), s^{1s}_{in}$,

$$
\begin{aligned}
F_{2s}[U(s)] = \left(\frac{1-U^2}{1-U_N^2}\right)^6 \Bigg\{ & \frac{1}{2}(\mu_p+\mu_n-1)H_{\omega''}(U)H_{\phi''}(U)H_{\omega'}(U) \\
& + \Bigg[H_{\phi''}(U)H_{\omega'}(U)H_{\phi'}(U)\frac{(C^{2s}_{\phi''}-C^{2s}_{\phi'})(C^{2s}_{\omega'}-C^{2s}_{\phi'})}{(C^{2s}_{\phi''}-C^{2s}_{\omega''})(C^{2s}_{\omega'}-C^{2s}_{\omega''})} \\
& + H_{\omega''}(U)H_{\omega'}(U)H_{\phi'}(U)\frac{(C^{2s}_{\omega''}-C^{2s}_{\phi'})(C^{2s}_{\omega'}-C^{2s}_{\phi'})}{(C^{2s}_{\omega''}-C^{2s}_{\phi''})(C^{2s}_{\omega'}-C^{2s}_{\phi''})} \\
& + H_{\omega''}(U)H_{\phi''}(U)H_{\phi'}(U)\frac{(C^{2s}_{\omega''}-C^{2s}_{\phi'})(C^{2s}_{\phi''}-C^{2s}_{\phi'})}{(C^{2s}_{\omega''}-C^{2s}_{\omega'})(C^{2s}_{\phi''}-C^{2s}_{\omega'})} \\
& - H_{\omega''}(U)H_{\phi''}(U)H_{\omega'}(U)\Bigg](f^{(2)}_{\phi' NN}/f_{\phi'}) \\
& + \Bigg[H_{\phi''}(U)H_{\omega'}(U)L_{\omega}(U)\frac{(C^{2s}_{\phi''}-C^{2s}_{\omega})(C^{2s}_{\omega'}-C^{2s}_{\omega})}{(C^{2s}_{\phi''}-C^{2s}_{\omega''})(C^{2s}_{\omega'}-C^{2s}_{\omega''})} \\
& + H_{\omega''}(U)H_{\omega'}(U)L_{\omega}(U)\frac{(C^{2s}_{\omega''}-C^{2s}_{\omega})(C^{2s}_{\omega'}-C^{2s}_{\omega})}{(C^{2s}_{\omega''}-C^{2s}_{\phi''})(C^{2s}_{\omega'}-C^{2s}_{\phi''})} + \\
& + H_{\omega''}(U)H_{\phi''}(U)L_{\omega}(U)\frac{(C^{2s}_{\omega''}-C^{2s}_{\omega})(C^{2s}_{\phi'}-C^{2s}_{\omega})}{(C^{2s}_{\omega''}-C^{2s}_{\omega'})(C^{2s}_{\phi''}-C^{2s}_{\omega'})} \\
& - H_{\omega''}(U)H_{\phi''}(U)H_{\omega'}(U)\Bigg](f^{(2)}_{\omega NN}/f_{\omega}) \\
& + \Bigg[H_{\phi''}(U)H_{\omega'}(U)L_{\phi}(U)\frac{(C^{2s}_{\phi''}-C^{2s}_{\phi})(C^{2s}_{\omega'}-C^{2s}_{\phi})}{(C^{2s}_{\phi''}-C^{2s}_{\omega''})(C^{2s}_{\omega'}-C^{2s}_{\omega''})} \\
& + H_{\omega''}(U)H_{\omega'}(U)L_{\phi}(U)\frac{(C^{2s}_{\omega''}-C^{2s}_{\phi})(C^{2s}_{\omega'}-C^{2s}_{\phi})}{(C^{2s}_{\omega''}-C^{2s}_{\phi''})(C^{2s}_{\omega'}-C^{2s}_{\phi''})} \\
& + H_{\omega''}(U)H_{\phi''}(U)L_{\phi}(U)\frac{(C^{2s}_{\omega''}-C^{2s}_{\phi})(C^{2s}_{\phi''}-C^{2s}_{\phi})}{(C^{2s}_{\omega''}-C^{2s}_{\omega'})(C^{2s}_{\phi''}-C^{2s}_{\omega'})} \\
& - H_{\omega''}(U)H_{\phi''}(U)H_{\omega'}(U)\Bigg](f^{(2)}_{\phi NN}/f_{\phi}) \Bigg\}
\end{aligned}
\tag{22}
$$

with 4 free parameters $(f^{(2)}_{\phi' NN}/f_{\phi'}), (f^{(2)}_{\omega NN}/f_{\omega}), (f^{(2)}_{\phi NN}/f_{\phi}), s^{2s}_{in}$,

$$
\begin{aligned}
F_{1v}[W(s)] = \left(\frac{1-W^2}{1-W_N^2}\right)^4 \Bigg\{ & \frac{1}{2}L_{\rho}(W)L_{\rho'}(W) \\
& + \Bigg[L_{\rho'}(W)L_{\rho''}(W)\frac{(C^{1v}_{\rho'}-C^{1v}_{\rho''})}{(C^{1v}_{\rho'}-C^{1v}_{\rho})} + L_{\rho}(W)L_{\rho''}(W)\frac{(C^{1v}_{\rho}-C^{1v}_{\rho''})}{(C^{1v}_{\rho}-C^{1v}_{\rho'})} \\
& - L_{\rho}(W)L_{\rho'}(W)\Bigg](f^{(1)}_{\rho NN}/f_{\rho}) \Bigg\}
\end{aligned}
\tag{23}
$$

 doi:10.20944/preprints202406.0383.v1

with 2 free parameters $(f^{(1)}_{\rho NN}/f_\rho)$ and s^{1v}_{in}, and

$$F_{2v}[X(s)] = \left(\frac{1-X^2}{1-X_N^2}\right)^6 \left\{\frac{1}{2}(\mu_p-\mu_n-1)L_\rho(X)L_{\rho'}(X)H_{\rho''}(X)\right\} \tag{24}$$

dependent on only 1 free parameter s^{2v}_{in}, where an explicit form of $V(s)$ is

$$V(s) = i\frac{\sqrt{(\frac{s^{1s}_{in}-s^s_0}{s^s_0})^{1/2}+(\frac{s-s^s_0}{s^s_0})^{1/2}}-\sqrt{(\frac{s^{1s}_{in}-s^s_0}{s^s_0})^{1/2}-(\frac{s-s^s_0}{s^s_0})^{1/2}}}{\sqrt{(\frac{s^{1s}_{in}-s^s_0}{s^s_0})^{1/2}+(\frac{s-s^s_0}{s^s_0})^{1/2}}+\sqrt{(\frac{s^{1s}_{in}-s^s_0}{s^s_0})^{1/2}-(\frac{s-s^s_0}{s^s_0})^{1/2}}}. \tag{25}$$

Similar expressions are used for $U(s), W(s)$ and $X(s)$ with $s^s_0 = 9m^2_\pi, s^v_0 = 4m^2_\pi$ the lowest square root branch points of the $F_{1s}(s), F_{2s}(s), F_{1v}(s), F_{2v}(s)$ functions and $s^{1s}_{in}, s^{2s}_{in}, s^{1v}_{in}, s^{2v}_{in}$ as effective inelastic square root branch points of these functions, effectively taking into account the contributions of all higher inelastic channels in the $e^+e^- \to hadrons$ processes. This construction defines the model on a 4-sheeted Riemann surface. The effective inelastic square root branch points are left to be free parameters of the model and their numerical values are evaluated in the analysis of the existing experimental data.

The lower L and the higher H notations have the following explicit forms

$$L_r(V) = \frac{(V_N-V_r)(V_N-V^*_r)(V_N-1/V_r)(V_N-1/V^*_r)}{(V-V_r)(V-V^*_r)(V-1/V_r)(V-1/V^*_r)}, \tag{26}$$
$$C^{1s}_r = \frac{(V_N-V_r)(V_N-V^*_r)(V_N-1/V_r)(V_N-1/V^*_r)}{-(V_r-1/V_r)(V_r-1/V^*_r)}, r = \omega, \phi$$

$$H_l(V) = \frac{(V_N-V_l)(V_N-V^*_l)(V_N+V_l)(V_N+V^*_l)}{(V-V_l)(V-V^*_l)(V+V_l)(V+V^*_l)}, \tag{27}$$
$$C^{1s}_l = \frac{(V_N-V_l)(V_N-V^*_l)(V_N+V_l)(V_N+V^*_l)}{-(V_l-1/V_l)(V_l-1/V^*_l)}, l = \omega'', \phi'', \omega', \phi'$$

$$L_k(W) = \frac{(W_N-W_k)(W_N-W^*_k)(W_N-1/W_k)(W_N-1/W^*_k)}{(W-W_k)(W-W^*_k)(W-1/W_k)(W-1/W^*_k)}, \tag{28}$$
$$C^{1v}_k = \frac{(W_N-W_k)(W_N-W^*_k)(W_N-1/W_k)(W_N-1/W^*_k)}{-(W_k-1/W_k)(W_k-1/W^*_k)}, k = \rho'', \rho', \rho$$

$$L_r(U) = \frac{(U_N-U_r)(U_N-U^*_r)(U_N-1/U_r)(U_N-1/U^*_r)}{(U-U_r)(U-U^*_r)(U-1/U_r)(U-1/U^*_r)}, \tag{29}$$
$$C^{2s}_r = \frac{(U_N-U_r)(U_N-U^*_r)(U_N-1/U_r)(U_N-1/U^*_r)}{-(U_r-1/U_r)(U_r-1/U^*_r)}, r = \omega, \phi$$

$$H_l(U) = \frac{(U_N-U_l)(U_N-U^*_l)(U_N+U_l)(U_N+U^*_l)}{(U-U_l)(U-U^*_l)(U+U_l)(U+U^*_l)}, \tag{30}$$
$$C^{2s}_l = \frac{(U_N-U_l)(U_N-U^*_l)(U_N+U_l)(U_N+U^*_l)}{-(U_l-1/U_l)(U_l-1/U^*_l)}, l = \omega'', \phi'', \omega', \phi'$$

Preprints.org (www.preprints.org) | NOT PEER-REVIEWED | Posted: 7 June 2024 doi:10.20944/preprints202406.0383.v1

$$L_k(X) = \frac{(X_N - X_k)(X_N - X_k^*)(X_N - 1/X_k)(X_N - 1/X_k^*)}{(X - X_k)(X - X_k^*)(X - 1/X_k)(X - 1/X_k^*)}, \tag{31}$$
$$C_k^{2v} = \frac{(X_N - X_k)(X_N - X_k^*)(X_N - 1/X_k)(X_N - 1/X_k^*)}{-(X_k - 1/X_k)(X_k - 1/X_k^*)}, k = \rho', \rho$$

$$H_{\rho''}(X) = \frac{(X_N - X_{\rho''})(X_N - X_{\rho''}^*)(X_N + X_{\rho''})(X_N + X_{\rho''}^*)}{(X - X_{\rho''})(X - X_{\rho''}^*)(X + X_{\rho''})(X + X_{\rho''}^*)}, \tag{32}$$
$$C_{\rho''}^{2v} = \frac{(X_N - X_{\rho''})(X_N - X_{\rho''}^*)(X_N + X_{\rho''})(X_N + X_{\rho''}^*)}{-(X_{\rho''} - 1/X_{\rho''})(X_{\rho''} - 1/X_{\rho''}^*)}.$$

They correspond to the case when the real part of the resonance location in the complex s-plane $m_r^2 - \Gamma_r^2/4 < s_{in}$ is below the effective inelastic square root branch point and to the case when the real part of the resonance location $m_r^2 - \Gamma_r^2/4 > s_{in}$ is found above the corresponding effective inelastic square root branch point, respectively.

A derivation of the U&A model of the nucleon EM structure can be found in detail in [17].

One finds the results of the fit of $\sigma_{tot}(e^+e^- \to p\bar{p})$ data [7]-[13] by means of the U&A model for the proton EM FFs in the Table III.

Table 3. Values of free parameters of the proton EM structure *U&A* model (21)-(32) from optimal description of $\sigma_{tot}(e^+e^- \to p\bar{p})$ data only.

$s_{in}^{1s} = (1.4279 \pm 0.0196)GeV^2; s_{in}^{1v} = (2.9240 \pm 0.0784)GeV^2;$
$s_{in}^{2s} = (1.8304 \pm 0.1764)GeV^2; s_{in}^{2v} = (2.6873 \pm 0.0784)GeV^2;$
$(f^{(1)}_{\omega' NN}/f_{\omega'}) = -0.0309 \pm 0.0084; (f^{(1)}_{\phi' NN}/f_{\phi'}) = -0.6423 \pm 0.0061;$
$(f^{(1)}_{\omega NN}/f_{\omega}) = 0.9970 \pm 0.0026; (f^{(1)}_{\phi NN}/f_{\phi}) = -0.0315 \pm 0.0010;$
$(f^{(2)}_{\phi' NN}/f_{\phi'}) = 0.7848 \pm 0.0183; (f^{(2)}_{\omega NN}/f_{\omega}) = -0.4967 \pm 0.1835;$
$(f^{(2)}_{\phi NN}/f_{\phi}) = 0.1490 \pm 0.0022; (f^{(1)}_{\rho NN}/f_{\rho}) = 0.1845 \pm 0.0037.$

With numerical values of the free parameters in Table III, one describes well all existing data on $\sigma_{tot}(e^+e^- \to p\bar{p})$ (see Figure 14a), including also a reproduction of the proton "effective" EM FF data Figure 1a. By means of the same U&A model [27] also the theoretically created pseudo-data (see later) together with the theoretically predicted curve for the neutron effective EM FF behavior are given in Figure 14b, by exchanging the EM FFs of the proton (19) in the U&A model by the neutron EM FFs (20).

The crucial moment in our investigations is the fact that the artificial neutron "effective" EM FF pseudo-data in Figure 14b are obtained from the data on $\sigma_{tot}(e^+e^- \to p\bar{p})$ only in the following way. First we evaluate deviations of the proton "effective"" EM FF data from the curve describing them in Figure 1b, by a subtraction of the curve from existing data. Then the obtained deviations are added to the theoretically predicted curve for the neutron "effective" EM FF in Figure 14b at the same energy value "s". As a result one obtains the 46 artificial points on the neutron "effective" EM FF data with errors from the proton "effective" EM FF data scattered around the theoretically predicted curve in Figure 14b, which also perfectly describes them.

We could, maybe in a more straightforward way, just show the smooth curve for the neutron effective FF as given by the U&A model. Here our motivation is to mimic the neutron data and their errors, although only very roughly by taking them from the proton case, all this to see what do the oscillations look like when some error estimates are present. Are they maybe insignificant when uncertainties are taken into the account?

 doi:10.20944/preprints202406.0383.v1

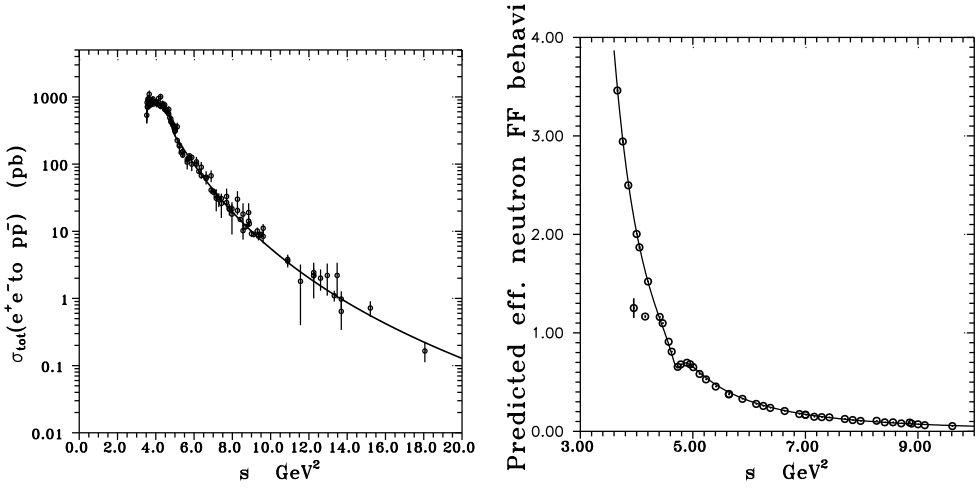

Figure 14. Fitted $\sigma_{tot}(e^+e^- \to p\bar{p})$ data with errors and their description by the U&A model 14a and theoretically created neutron effective EM FF pseudo-data by the same U&A model 14b, however with a change of (19) to (20).

When such artificially created pseudo-data on the neutron "effective" EM FF are described by the three parametric function (5) with values of the parameters $A(1) = 1.0971 \pm 0.0879$, $m_a^2 = 6.1112 \pm 0.6670$ GeV^2, $A(3) = 2.5321 \pm 9,9162$ GeV^2 the RDOS appear as it is seen in Figure 15 and they are just opposite to the proton RDOS in Figure 2 from the proton "effective" EM FF data in Figure 1a.

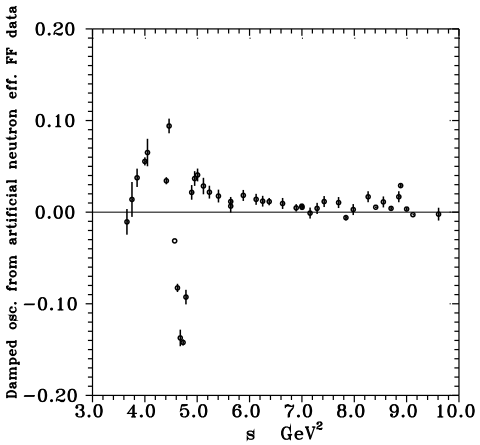

Figure 15. The result of the subtraction of the curve in Figure 14b from the neutron “effective” FF data with errors demonstrates damped oscillation regular structures just opposite to the oscillations from the proton "effective" EM FF data.

As the artificial pseudo-data on the neutron "effective" EM FF have been obtained from the proton "effective" EM FF data only by means of the U&A analytic model (same for the proton and neutron) through the relations (19) and (20), which reflect explicitly the special transformation of the nucleon EM current in the isospin space, we come to the conclusion that the origin of the phenomenon of the oppositely RDOS behaviors for protons and neutrons is in the special transformations of the nucleon EM current in the isotopic space.

The justification for not using the existing experimental neutron data is that these are not good enough in quantity and quality to allow reliable fits in the U&A model. Rather we adopt the following logic: We observe the "opposite oscillatory" behavior in the true neutron data (when compared to the proton data) and then we reproduce this opposite oscillatory feature (not individual data points) in the U&A model-generated pseudo-data by taking into consideration the isospin structure. Because we succeed in the reproduction of this phenomenon, we draw the above-presented conclusions.

Preprints.org (www.preprints.org) | NOT PEER-REVIEWED | Posted: 7 June 2024 doi:10.20944/preprints202406.0383.v1

9. Description of Hadron "Effective" FF Data by Means of the Unitary&Analytic Approach

If the same data on the considered hadron "effective" FFs are described by slightly more complicated, however, physically well founded, the universal Unitary and Analytic (U&A) models [17] of their EM structure, no damped oscillation regular structures appear. As the data of all considered hadrons are not of the same quality, also the corresponding U&A models are specific from one case to the other.

9.1. Description of the Charged Pion "Effective" EM FF Data by Means of the U&A Model

The application of the U&A model, Eqs. (7)-(10) with parameters from Table I, to the data on $G^{\pi^{\pm}}_{eff}(s) = |F^{c}_{\pi}(s)|$, summarized in Table.II-Table IV of [4], leads to a perfect description of the latter as shown by the full line in Figure 16. If these full line data in Figure 16 are subtracted from the data in Table.II-Table IV of [4], no oscillatory regular structures appear as it is clearly seen in Figure 17.

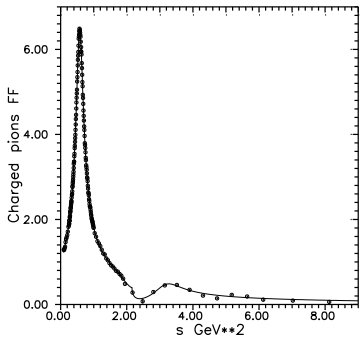

Figure 16. The optimal description of $|F^{c}_{\pi}(s)|$ data by the U&A model (7)-(10) and parameters values of Table I as given by the full line.

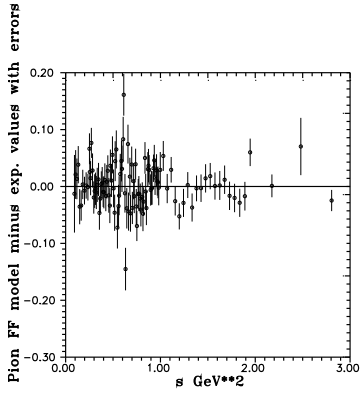

Figure 17. The subtraction of the full line in Figure 16 from the pure EM form factor $|F^{c}_{\pi}(s)|$ data as given in Table.II-Table IV of [4] reveal no RDOS.

9.2. Description of the proton "effective" EM FF data by means of the U&A model

To describe the "effective" proton FF in the U&A model, we substitute the explicit form of the proton total cross section (1) into the expression (3). Then the relation between the absolute values of the complex proton EM FFs squared, represented by means of the U&A model and the proton "effective" FF (3) is found

$$G^{p}_{eff}(s) = \sqrt{\frac{\left[|G^{p}_{M}(s)|^2 + \frac{2m_p^2}{s}|G^{p}_{E}(s)|^2\right]}{\left(1 + \frac{2m_p^2}{s}\right)}} \tag{33}$$

Preprints.org (www.preprints.org) | NOT PEER-REVIEWED | Posted: 7 June 2024 doi:10.20944/preprints202406.0383.v1

and the description of the data on the proton "effective" FF data with $\chi^2/ndf = 1.85$ (see Figure 18) is achieved.

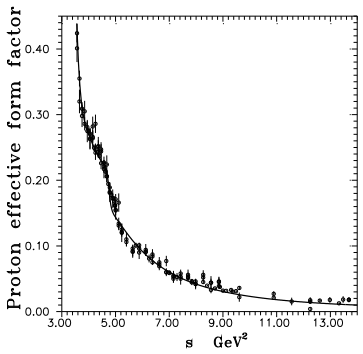

Figure 18. The description of the proton "effective" FF data in Figure 1 by the *U&A* model (21)-(24) with the numerical values of the parameters given in Table III.

Then the subtraction of the curve of Figure 18 from the proton's "effective" FF data with errors demonstrates no RDOS, as it is clearly seen in Figure 19.

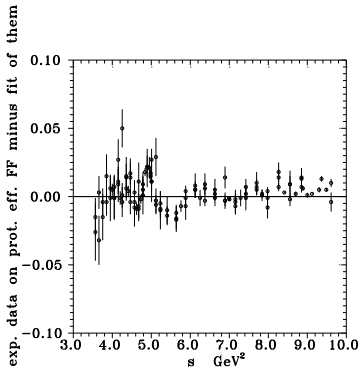

Figure 19. The result of a subtraction of the curve in Figure 18 from the proton "effective" FF data with errors demonstrates no RDOS.

9.3. Description of the Neutron "Effective" FF Data by Means of the U&A Model

Similarly to the proton, also for the neutron one can derive the relation

$$G^n_{eff}(s) = \sqrt{\frac{\left[|G^n_M(s)|^2 + \frac{2m_n^2}{s}|G^n_E(s)|^2\right]}{\left(1+\frac{2m_n^2}{s}\right)}} \tag{34}$$

between the neutron EM FFs represented by means of the U&A model and the neutron "effective" FF (4). Then accurately describing the neutron "effective" FF data in Figure 3a as it is demonstrated in Figure 20 and subtracting the fitted curve from the data on the neutron "effective" FF , one finds some structures (see Figure 21), from which, however, one can not conclude about the (non)existence of RDOS. In order to obtain a definitive statement, more precise data on $e^+e^- \to n\bar{n}$ are needed.

Preprints.org (www.preprints.org) | NOT PEER-REVIEWED | Posted: 7 June 2024 doi:10.20944/preprints202406.0383.v1

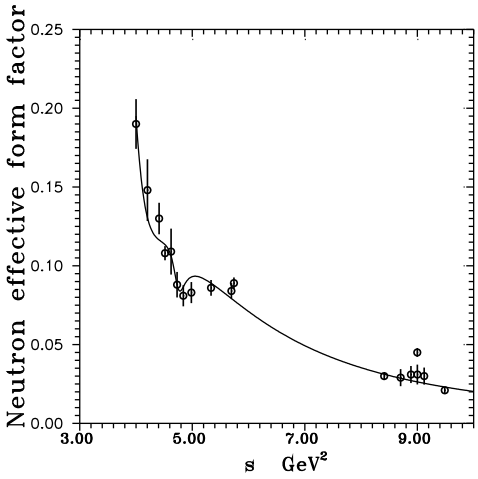

Figure 20. The description of the neutron "effective" FF data in Figure 3a by the *U&A* model (21)-(24) with the numerical values of the parameters in Table IV.

Table 4. Values of free parameters of the neutron EM structure *U&A* model (21)-(32) from optimal description of the neutron "effective" FF data in Figure 3a.

$$s_{in}^{1s} = (2.2188 \pm 0.0053)GeV^2; s_{in}^{1v} = (6.0930 \pm 0.0002)GeV^2;$$
$$s_{in}^{2s} = (3.2748 \pm 0.0009)GeV^2; s_{in}^{2v} = (5.6194 \pm 0.0067)GeV^2;$$
$$(f^{(1)}_{\omega' NN}/f_{\omega'}) = 2.2045 \pm 0.0172; (f^{(1)}_{\phi' NN}/f_{\phi'}) = -0.5700 \pm 0.0028;$$
$$(f^{(1)}_{\omega NN}/f_{\omega}) = 0.10903 \pm 0.0022; (f^{(1)}_{\phi NN}/f_{\phi}) = 0.17613 \pm 0.0001;$$
$$(f^{(2)}_{\phi' NN}/f_{\phi'}) = -.7089 \pm 0.0002; (f^{(2)}_{\omega NN}/f_{\omega}) = 0.oo32 \pm 0.0001;$$
$$(f^{(2)}_{\phi NN}/f_{\phi}) = 0.0001 \pm 0.0001; (f^{(1)}_{\rho NN}/f_{\rho}) = 0.1314 \pm 0.0001.$$

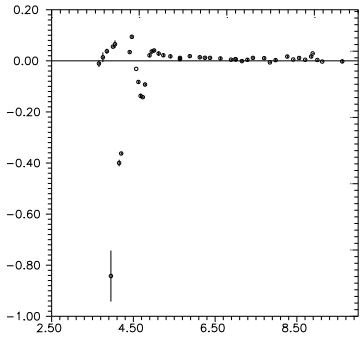

Figure 21. The result of a subtraction of the curve in Figure 20 from the neutron "effective" FF data with errors indicates no damped oscillation regular structures.

9.4. Description of the Charged K-Meson "Effective" EM FF Data by Means of the U&A Model

Here we will show that when charged K-meson data in Figure 7 are accurately described by an appropriate physically well founded U&A model of the K-meson EM structure, no damped oscillatory structures are observed.

We will use the model that has been suggested in the paper [17] as the universal U&A EM structure model of hadrons and which unifies three aspects:

1. Experimental fact of the creation of unstable vector-meson resonances (see [18]), mainly identified in the electron-positron annihilation processes into hadrons.
2. Two square root branch cut approximation of the analytic properties of FFs in the complex plane of c.m. energy squared s.
3. The correct asymptotic behavior of FFs as predicted by the quark model of hadrons.

 doi:10.20944/preprints202406.0383.v1

To describe the selected data in Figure 7 in the framework of the U&A approach [17] we begin by splitting the charged K-meson FF in accordance with the special transformation properties of the K-meson EM current in the isospin space, into a sum of the isoscalar and isovector parts

$$F_{K^\pm}(s) = F_K^s(s) + F_K^v(s) \tag{35}$$

with their norms

$$F_K^s(0) = F_K^v(0) = \frac{1}{2}. \tag{36}$$

Next we must deal with the question of what isoscalar and isovector resonances experimentally confirmed in [18] will saturate the isoscalar and isovector parts of the charged kaon FF. In practice one can not consider all existing resonances with isospin $I = 0$ and isospin $I = 1$, as they will produce all together 25 free parameters, too much to be evaluated in the analysis of up-to-date existing experimental information. As a result a selection of contributing resonances has to be carried out and is done in the following way.

The K-mesons consist also of the strange quarks, therefore one could expect that in a description of the selected data in Figure 7 and Figure 8 all three ϕ resonances with the isospin $I = 0$ will be dominant and therefore the masses and widths of $\phi(1020)$ and $\phi(1680)$ will be left as free parameters of the model. Only the parameters of $\phi(2170)$ will be fixed at the PDG values, since in the corresponding energy region the analyzed data are insufficient. There is no doubt about the inclusion of the $\phi(1020)$ resonance clearly seen in Figure 7. From Figure 7 (in more detail in Figure 8) between 2.0 GeV^2 and 7.0 GeV^2 one finds two bumps corresponding approximately to $\phi'(1680)$ and $\phi''(2170)$. The first bump could contain a contribution also from another resonance with $I = 0$, $\omega''(1650)$, which is therefore not excluded. There is no indication in existing data of a contribution of $\omega'(1420)$, therefore we don't consider it in our analysis.

On the other hand we have an experience that one can not achieve satisfactory description of existing data without inclusion of the ground state resonances $\rho(770)$ and $\omega(782)$. Further, because contributions of the isovector part of the K-meson FF, though not dominant, can not be ignored, we include contributions of all three ρ-mesons, however with fixed parameters from the paper [22], in which one can find reasons why not to use their parameters from [18]. Masses and widths of $\omega(782)$ and $\omega''(1650)$ are also fixed at the PDG values.

Then the U&A model of the K-meson EM structure takes the following form. The isoscalar FF with 5 experimentally confirmed [18] isoscalar resonances is

$$\begin{aligned} F_K^s[V(s)] &= \left(\frac{1-V^2}{1-V_N^2}\right)^2 \\ &\times \Big[\sum_{s=\omega,\phi} \frac{(V_N - V_s)(V_N - V_s^*)(V_N - 1/V_s)(V_N - 1/V_s^*)}{(V - V_s)(V - V_s^*)(V - 1/V_s)(V - 1/V_s^*)} \left(\frac{f_{sKK}}{f_s}\right) \\ &+ \sum_{s=\phi',\omega'',\phi''} \frac{(V_N - V_s)(V_N - V_s^*)(V_N + V_s)(V_N + V_s^*)}{(V - V_s)(V - V_s^*)(V + V_s)(V + V_s^*)} \left(\frac{f_{sKK}}{f_s}\right)\Big], \end{aligned} \tag{37}$$

where the concrete form of individual terms depends on the numerical value of the effective inelastic threshold s_{in}^s which is found numerically by the fit of the model to charged K-meson EM FF selected data. In the previous expression

$$V(s) = i\frac{\sqrt{\left(\frac{s_{in}^s - s_0^s}{s_0^s}\right)^{1/2} + \left(\frac{s - s_0^s}{s_0^s}\right)^{1/2}} - \sqrt{\left(\frac{s_{in}^s - s_0^s}{s_0^s}\right)^{1/2} - \left(\frac{s - s_0^s}{s_0^s}\right)^{1/2}}}{\sqrt{\left(\frac{s_{in}^s - s_0^s}{s_0^s}\right)^{1/2} + \left(\frac{s - s_0^s}{s_0^s}\right)^{1/2}} + \sqrt{\left(\frac{s_{in}^s - s_0^s}{s_0^s}\right)^{1/2} - \left(\frac{s - s_0^s}{s_0^s}\right)^{1/2}}} \tag{38}$$

 doi:10.20944/preprints202406.0383.v1

is the conformal mapping of the four sheeted Riemann surface into one V-plane, and $V_N = V(0)$ is a normalization point in the V-plane with $s_0^s = 9m_\pi^2$. The isovector FF with 3 experimentally confirmed [18] isovector resonances $\rho(770), \rho'(1450), \rho''(1700)$ takes the form

$$F_K^v[W(s)] = (\frac{1-W^2}{1-W_N^2})^2[\frac{(W_N-W_\rho)(W_N-W_\rho^*)(W_N-1/W_\rho)(W_N-1/W_\rho^*)}{(W-W_\rho)(W-W_\rho^*)(W-1/W_\rho)(W-1/W_\rho^*)}(\frac{f_{\rho\pi\pi}}{f_\rho}) + \sum_{v=\rho',\rho''}\frac{(W_N-W_v)(W_N-W_v^*)(W_N+W_v)(W_N+W_v^*)}{(W-W_v)(W-W_v^*)(W+W_v)(W+W_v^*)}(\frac{f_{v\pi\pi}}{f_v})], \quad (39)$$

and again the structure of individual terms depends on the value of the effective inelastic threshold s_{in}^v numerically evaluated in the fitting procedure of the model to charged K-meson EM FF data. In the previous expression

$$W(s) = i\frac{\sqrt{(\frac{s_{in}^v-s_0^v}{s_0^v})^{1/2}+(\frac{s-s_0^v}{s_0^v})^{1/2}}-\sqrt{(\frac{s_{in}^v-s_0^v}{s_0^v})^{1/2}-(\frac{s-s_0^v}{s_0^v})^{1/2}}}{\sqrt{(\frac{s_{in}^v-s_0^v}{s_0^v})^{1/2}+(\frac{s-s_0^v}{s_0^v})^{1/2}}+\sqrt{(\frac{s_{in}^v-s_0^v}{s_0^v})^{1/2}-(\frac{s-s_0^v}{s_0^v})^{1/2}}} \quad (40)$$

is a conformal mapping of the four sheeted Riemann surface, on which $F_K^v(s)$ is defined, into one W-plane, and $W_N = W(0)$ is a normalization point in the W-plane, with $s_0^v = 4m_\pi^2$.

As a result, the U&A model of the K-meson EM structure depends altogether on 14 free parameters and their numerical values (see Table V) have been evaluated in the analysis of selected data from Figure 7.

Table 5. Parameter values of the U&A model in the analysis of selected data on $|F_{K^\pm}(s)|$ with minimum of $\chi^2/ndf = 1.79$

$s_{in}^s = (1.0984 \pm 0.2292)$ [GeV^2];
$m_\phi = (1019.298 \pm 0.063)$ [MeV]; $\Gamma_\phi = (4.304 \pm 0.083)$ [MeV]; $(f_{\phi KK}/f_\phi) = 0.331 \pm 0.063$;
$m_{\phi'} = (1656.620 \pm 4.969)$ [MeV]; $\Gamma_{\phi'} = 356.860 \pm 4.444)$ [MeV]; $(f_{\phi' KK}/f_{\phi'}) = -.568 \pm 0.102$;
$m_{\phi''} = (2001.300 \pm 22.817)$ [MeV]; $\Gamma_{\phi''} = (530.502 \pm 34.300)$ [MeV];
$(f_{\phi'' KK}/f_{\phi''}) = 1/2 - (f_{\omega KK}/f_\omega) - (f_{\omega'' KK}/f_{\omega''}) - (f_{\phi KK}/f_\phi) - (f_{\phi' KK}/f_{\phi'})$;
$(f_{\omega KK}/f_\omega) = 0.273 \pm 0.044$; $(f_{\omega'' KK}/f_{\omega''}) = 0.354 \pm 0.103$;
$s_{in}^v = (1.6765 \pm 0.1337)$ [GeV^2];
$(f_{\rho' KK}/f_{\rho'}) = 1/2 - (f_{\rho KK}/f_\rho) - (f_{\rho'' KK}/f_{\rho''})$;
$(f_{\rho KK}/f_\rho) = 0.440 \pm 0.017$; $(f_{\rho'' KK}/f_{\rho''}) = 0.036 \pm 0.005$;

The corresponding accurate description of these charged K-meson EM FF data is presented in Figure 22 by the full line. One finds the description of the resonant region between 2.0 GeV^2 and 7.0 GeV^2 in more detail in Figure 23.

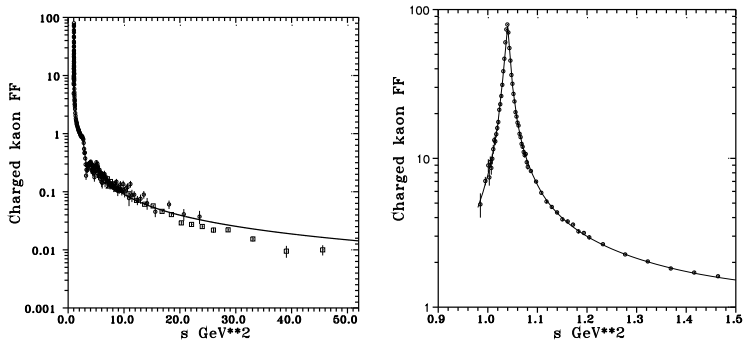

Figure 22. Charged kaon EM FF data described by the U&A model.

Preprints.org (www.preprints.org) | NOT PEER-REVIEWED | Posted: 7 June 2024 doi:10.20944/preprints202406.0383.v1

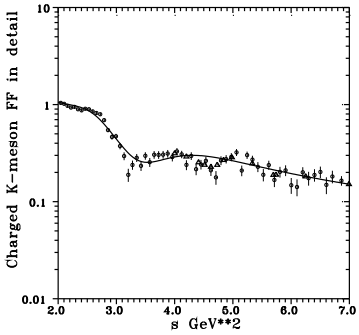

Figure 23. Description of charge K-meson EM FF data by the U&A model between 2.0 GeV^2 and 7.0 GeV^2.

Lastly, if the full line in Figure 22 is subtracted from selected charged K-meson FF data in Figure 7 with errors, no damped oscillatory structures are observed around the line crossing the zero as it is shown in Figure 24.

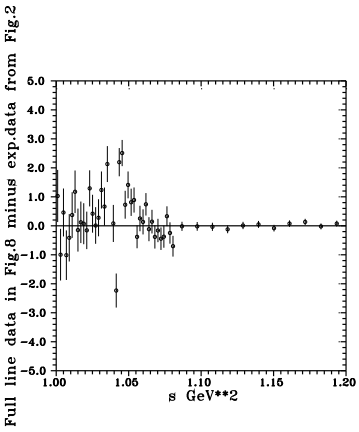

Figure 24. No damped oscillatory structures appear if $|F_{K^\pm}(s)|$ data are accurately described by the U&A model of K-meson EM structure as presented in Figure 22.

9.5. Description of the Neutral K-Meson "Effective" EM FF Data by Means of the U&A Model

Now, as in the case of the charged K-meson EM FF data, we shall try to demonstrate that if neutral K-meson EM FF data in Figure 25 are accurately described by a proper physically well founded U&A model, no damped oscillatory structures are observed.

The simplest way to obtain such a description is to exploit the special transformation properties of the K-meson EM current in the isospin space, from which it directly follows that we can write the neutral K-meson EM FF as the difference of the isoscalar and isovector parts

$$F_{K^0}(s) = F_K^s(s) - F_K^v(s) \tag{41}$$

where $F_K^s(s)$ and $F_K^v(s)$ are the same as those in (35). The charged and neutral K-meson EM FFs then depend on the same set of parameters of the *U&A* model.

Thus a substitution of the numerical values of parameters from Table V into the K-meson EM FF U&A model (37)-(40) should lead through (41) to an accurate description of data in Table II.

However, as it can be explicitly seen in Figure 25 by looking at the dotted line, especially in the energy region from 1.4 GeV^2 up to 6.0 GeV^2, the predicted behavior does not follow the data for $|F_{K^0}(s)|$ accurately.

There are several ways how to interpret this discrepancy. It can be a demonstration of the non exact conservation of the isospin symmetry or some subtle error in the definition of the isoscalar and isovector parts in the *U&A* model. Furthermore, it is possible that the data are not precise enough

 doi:10.20944/preprints202406.0383.v1

to allow for a good separation of the isoscalar and isovector components by a fitting procedure on charged kaon data only (as opposed to fitting on both the charged and neutral kaon data together). And lastly, it could be that the two experimental data sets are simply inconsistent. Nevertheless, resolving this issue is not important for the purpose of the current article.

So, in order to achieve an accurate description of data in Table II and to look for damped oscillatory structures from the neutral K-meson EM FF timelike data, one has to carry out a direct fitting procedure of the latter data by the K-meson EM FF *U&A* model (37)-(40). This yields the 14 parameters whose numerical values are presented in Table VI. These parameters differ from parameter values in Table V. This may indicate that the data on the charged K-meson EM FF and the data on the neutral K-meson EM FF are really inconsistent.

The most accurate description of the $|F_{K^0}(s)|$ data corresponding to the parameters in Table VI is graphically presented in Figure 25 by the full line.

Table 6. Parameter values from the analysis of selected data on $|F_{K^0}(s)|$ by the K-meson EM FF U&A model (37)-(40) with minimum of $\chi^2/ndf = 4.37$.

$$s^s_{in} = (2.0728 \pm 0.0196)\ [\mathrm{GeV}^2];$$
$$m_\phi = (1019.158 \pm 0.176)\ [\mathrm{MeV}];\ \Gamma_\phi = (4.214 \pm 0.030)\ [\mathrm{MeV}];\ (f_{\phi KK}/f_\phi) = 0.336 \pm 0.001;$$
$$m_{\phi'} = (1649.760 \pm 5.356)\ [\mathrm{MeV}];\ \Gamma_{\phi'} = 340.032 \pm 12.438)\ [\mathrm{MeV}];\ (f_{\phi' KK}/f_{\phi'}) = -.217 \pm 0.001;$$
$$m_{\phi''} = (2028.740 \pm 46.556)\ [\mathrm{MeV}];\ \Gamma_{\phi''} = (383.418 \pm 45.489)\ [\mathrm{MeV}];$$
$$(f_{\phi'' KK}/f_{\phi''}) = 1/2 - (f_{\omega KK}/f_\omega) - (f_{\omega'' KK}/f_{\omega''}) - (f_{\phi KK}/f_\phi) - (f_{\phi' KK}/f_{\phi'});$$
$$(f_{\omega KK}/f_\omega) = 0.278 \pm 0.001;\ (f_{\omega'' KK}/f_{\omega''}) = 0.088 \pm 0.001;$$
$$s^v_{in} = (2.0077 \pm 0.0785)\ [\mathrm{GeV}^2];$$
$$(f_{\rho' KK}/f_{\rho'}) = 1/2 - (f_{\rho KK}/f_\rho) - (f_{\rho'' KK}/f_{\rho''});$$
$$(f_{\rho KK}/f_\rho) = 0.606 \pm 0.004;\ (f_{\rho'' KK}/f_{\rho''}) = -.044 \pm 0.010;$$

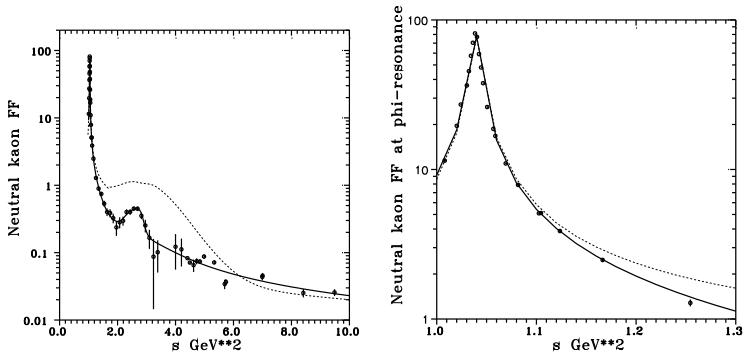

Figure 25. Neutral kaon EM FF data described by the full line to be obtained by K-meson EM FF U&A model (37)-(40) with parameters of Table VI.

If full line in Figure 25 is subtracted from selected neutral K-meson EM FF data in Table II taking into the account the errors, one obtains points and their uncertainties around the line crossing the zero in Figure 26, which clearly demonstrate the absence of RDOS.

 doi:10.20944/preprints202406.0383.v1

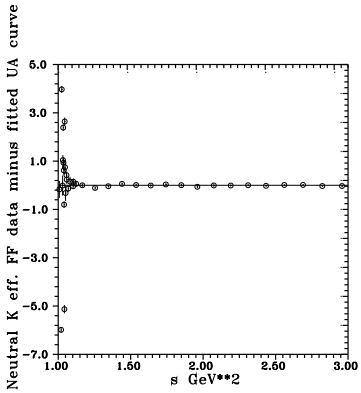

Figure 26. Points with errors obtained by a subtraction of full line data in Figure 25 from $|F_{K^0}(s)|$ data with errors in Table II.

The authors acknowledge the support of the Slovak Grant Agency for Sciences VEGA, grant No.2/0105/21.

10. Conclusions and Discussion

The RDOS from the proton "effective" form factor data in [1] raised a wide interest to study the damped oscillatory structures from the EM FFs data of other hadrons, for which solid data together with a physically well founded model for their accurate description exist.

In this work the problem of the existence of the RDOS regarding the charged pion and the charged and neutral K-meson EM FF data and also data on the neutron EM FF has been investigated using the same procedure as the one used in the case of the proton in [1].

When the "effective" data of the considered hadrons are described by the three parametric function of [9], the regular damped oscillatory structures appear. However, if for a description of the same data more physically founded U&A model of the EM structure of hadrons is applied, no regular damped oscillatory structures appear.

So, the results of all these investigations indicate that there is no objective existence of RDOS from the "effective" hadron EM FF data and their appearance is due to application of the three parametric formula [9] without any physical background to be unable to describe the latter data with the adequate accuracy. Moreover, our U&A model shows its capabilities to be applicable for description of a wide range of hadronic processes.

Acknowledgments: The authors acknowledge the support of the Slovak Grant Agency for Sciences VEGA, grant No.2/0105/21.

References

1. A.Bianconi, E.Tomasi-Gustafsson, Phys. Rev. Lett. **114**, 232301 (2015).
2. M. Ablikim et al., Nature Phys. **17**, 1200 (2021).
3. E.Tomasi-Gustafsson, S.Pacetti, Phys. Rev. **C106**, 035203 (2022).
4. E.Bartos, S.Dubnicka, A.Z.Dubnickova, Dynamics **3**(1), 137 (2023).
5. S.Dubnicka, A.Z.Dubnickova, L.Holka, A.Liptaj, Eur. Phys. J. **A59**, 190 (2023).
6. R.Baldini Ferroli, S.Pacetti, A.Zallo, Eur. Phys. J. **A48**, 33 (2012).
7. J.P.Lees et al,(BABAR Collab.) Phys. Rev. **D87**, 092005 (2013).
8. J.P.Lees et al,(BABAR Collab.) Phys. Rev. **D88**, 072009 (2013).
9. E. Tomasi-Gustafsson, M. P. Rekalo, Phys. Lett. **B504**, 291 (2001).
10. M. Ablikim et al., Phys. Rev. **D91**, 112004 (2015).
11. M. Ablikim et al., Phys. Rev. **D99**, 092002 (2019).
12. M. Ablikim et al., Phys. Rev. Lett. **124**, 042001 (2020).
13. M. Ablikim et al., Phys. Lett. **B817**, 136328 (2021).
14. J.P.Lees et al., Phys. Rev. **D86**, 032013 (2012).

 doi:10.20944/preprints202406.0383.v1

15. T.Xiao et al., Phys. Rev. **D97**, 032012 (2018).
16. M.Ablikim et al., Phys. Lett. **B812**, 135982 (2021).
17. S.Dubnicka, A.Z.Dubnickova, Acta Phys. Slovaca 60, 1 (2010).
18. P.A.Zyla et al., PTEP **2020**, 083C01 (2020).
19. M.E.Biagini, S.Dubnicka, E.Etim, P.Kolar, Nuovo Cim **A104**, 363 (1991).
20. S.Dubnicka, V.A.Meshcheryakov, J.Milko, J. Phys. G **7**, 605 (1981).
21. R.Garcia, R.Kaminski, J.R.Pelaez, J.Ruiz de Elvira, F.J.Yndurain, Phys. Rev. **D83**, 074004 (2011).
22. E.Bartos, S.Dubnicka, A.Liptaj, A.Z.Dubnickova, R.Kaminski, Phys. Rev. **D96**, 113004 (2017).
23. J.P.Lees et al., Phys. Rev. **D88**, 032013 (2013).
24. J.P.Lees et al., Phys. Rev. **D92**, 072008 (2015).
25. J.P.Lees et al., Phys. Rev. **D89**, 092002 (2014).
26. E.A.Kozyrev et al, Phys. Lett. **B760**, 314 (2016).
27. C.Adamuscin, E.Bartos, S.Dubnicka, A.Z.Dubnickova, Phys. Rev. **C93**, 055208 (2016).